

Stabilizer Rényi Entropy for Translation-Invariant Matrix Product States

Lei-Yi-Nan Liu,¹ Su Yi,^{2,3} and Jian Cui^{1,*}

¹*School of Physics, Beihang University, Beijing 100191, China*

²*Institute of Fundamental Physics and Quantum Technology & School of Physical Science and Technology, Ningbo University, Ningbo, 315211, China*

³*Peng Huanwu Collaborative Center for Research and Education, Beihang University, Beijing 100191, China*

(Dated: August 6, 2025)

Magic, capturing the deviation of a quantum state from the stabilizer formalism, is a key resource underpinning the quantum advantage. The recently introduced stabilizer Rényi entropy (SRE) offers a tractable measure of magic, avoiding the complexity of conventional methods. We study SRE in translation-invariant matrix product states (MPS), deriving exact expressions for representative states and introducing a numerically stable algorithm, named bond-DMRG, to compute the SRE density in infinite systems. Applying this method, we obtain high-precision SRE densities for the ground state of the one-dimensional Ising model. We also analyze non-local SRE density, showing it is bounded by a universal function of entanglement entropy, and further prove that two-site mutual SRE vanishes asymptotically in injective MPS. Our work not only introduces a powerful method for extracting the SRE density in quantum many-body systems, but also numerically reveals a fundamental connection between magic and entanglement, thereby paving the way for deeper theoretical investigations into their interplay.

I. INTRODUCTION

Quantum entanglement, which captures the non-classical correlation between different degrees of freedom within a quantum state [1], plays a fundamental role in unraveling collective phenomena. These range from quantum phase transitions [2], superconductivity [3], many-body localization [4] to the emergence of exotic phases, including (symmetry-protected) topological phases, spin liquids and other nontrivial quantum states [5–8]. From a practical applications perspective, it is also instrumental in both quantum computation and the design of classical computational algorithms. In quantum circuits, entanglement serves as a key resource that enables quantum algorithms to surpass classical computational capabilities [9, 10]. It also underpins quantum error correction techniques, ensuring the robustness and reliability of quantum computations [11]. In the classical realm, analyzing entanglement enables the development of tensor network representation for quantum many-body states. They serve as a powerful ansatz for numerically simulating the slightly entangled quantum many-body systems with the density matrix renormalization group method [12, 13].

Notice that mere entanglement alone is insufficient to guarantee the supremacy of quantum computation over its classical counterpart. As the Gottesman-Knill theorem demonstrates, certain highly entangled quantum systems are amenable to efficient classical simulation [14]. This theorem asserts that quantum circuits comprising only qubits prepared in computational-basis, Clifford gates, and classical measurements are perfectly simulable in polynomial time on a probabilistic classical computer. These specific quantum states, known as

stabilizer states, form the orbit of the Clifford group, which is the normalizer of the Pauli group. The capacity to transcend the Gottesman-Knill theorem represents a critical resource, commonly termed non-Cliffordness, non-stabilizerness, or more concisely, *magic* [15]. Standard measures of magic are typically grounded in general resource theory considerations, such as their invariance under Clifford operations and their faithfulness, meaning they vanish for stabilizer states. However, most of these measures either involve optimizing over all possible stabilizer decompositions of a state, which is computationally difficult, or they do not lend themselves to a direct interpretation as expectation values of an observable [15–21]. Recent advancements have introduced a novel measure of magic, namely the stabilizer Rényi entropy (SRE), which circumvents the need for a minimization procedure [22]. Nevertheless, for an n -qubit state, the calculation of the SRE remains a formidable challenge, as it necessitates evaluating 4^n Pauli strings, rendering exact computation infeasible for $n \gtrsim 17$. Thus, it is highly demanding to develop efficient methods to evaluate SRE for large-scale quantum systems.

It is of significant importance to explore the relationship between entanglement and magic, both of which are fundamental resources for quantum computation. Traditionally, these quantities have been regarded as distinct and largely uncorrelated: stabilizer states can exhibit high entanglement despite having zero magic, while product states can possess significant magic without entanglement. This distinction arises because entanglement is invariant under local unitary transformations, whereas magic is sensitive to both local and non-local transformations. However, recent work demonstrate that magic correlates strongly with the structure of entanglement [23], and that their interplay can induce Hilbert space fragmentation and computational phase transitions [24]. This naturally raises the question: what remains if one

* jiancui@buaa.edu.cn

removes the contribution from local unitaries and focuses solely on the non-local component of magic, and how does it relate to entanglement? To address this, in this paper we define and investigate the non-local SRE density, aiming to reveal its connection to entanglement entropy.

Going one step further, it is interesting to integrate entanglement and magic for advancing quantum information processing architectures and designing novel tools to probe and simulate complex quantum many-body systems. For matrix product states (MPS) using DMRG the complexity of computing SRE can be significantly reduced to polynomial time [25, 26]. Despite this advantage, existing studies of SRE are largely restricted to finite-size systems. For instance, in one-dimensional Ising model, the computed SRE density typically exhibits a peak that deviates slightly from the actual critical point due to finite-size effects [25, 26]. In models with known phase transition points, finite-size scaling techniques can sometimes be used to argue that the SRE density peak converges to the critical point in the thermodynamic limit. However, such extrapolations are generally unreliable for more complex or less understood models. In fact, it has been observed that full-state magic is not universally aligned with criticality [27], suggesting that even in the infinite-size limit, the SRE density peak may not coincide with the critical point. Finite-size effects may thus lead to a misleading picture of how SRE behaves near phase transitions, potentially obscuring valuable or subtle physical phenomena. Moreover, increasing the system size leads to rapidly growing computational costs and often reduced numerical precision due to the accumulation of statistical or truncation errors. These limitations hinder the accurate characterization of SRE near criticality using finite systems. To overcome these challenges, it is crucial to develop methods that directly access the thermodynamic limit. This motivates our focus on translationally invariant matrix product states (TIMPS), which provide a natural framework for describing infinite one-dimensional quantum systems.

In this paper, we first present a framework for computing the SRE in TIMPS, and derive analytical expressions for the SRE of several representative states, including spin-coherent product states, GHZ-like states, W states, and Dicke states, each of which plays a significant role in quantum information and quantum computation [28–32]. To overcome the limitations of finite-size approaches discussed above, we extend our analysis to infinite MPS (iMPS). Existing algorithms for finite MPS, however, often suffer from numerical instability when directly applied to iMPS. To address this challenge, we introduce bond-DMRG, a stable and efficient method specifically designed to compute the SRE density for iMPS with high precision. Using this approach, we compute the SRE density of the ground state of the one-dimensional Ising model with state-of-the-art precision, and show that in this model, the SRE density indeed peaks at the critical point. We further explore the behavior of both local and non-local SRE densities across different ensembles of ran-

dom iMPS. Finally, we study the mutual SRE (mSRE) as a measure of non-local magic. We prove that mSRE vanishes asymptotically for injective iMPS in the long-range limit, and demonstrate this in the Ising model, where the mSRE not only decays rapidly but also exhibits non-analytic behavior in its derivative at the critical point under unbroken \mathbb{Z}_2 symmetry.

II. SRE FOR TIMPS

The α -stabilizer Rényi entropy (α -SRE) for a n -qubit pure state $|\psi\rangle$ is defined as

$$M_\alpha(|\psi\rangle) := \frac{1}{1-\alpha} \log \sum_{P \in \mathcal{P}_n} \Xi_P^\alpha(|\psi\rangle) - \log d \quad (1)$$

where \mathcal{P}_n is the group of all n -qubit Pauli strings with $+1$ phase, and $\Xi_P(|\psi\rangle) := d^{-1} \langle \psi | P | \psi \rangle^2$ with $d = 2^n$ the dimension of n -qubit Hilbert space [22]. From the perspective of resource theory, for Rényi index $0 \leq \alpha < 2$, the SRE are not monotones with respect to stabilizer protocols which include computational-basis measurement, that is, these SRE are not reliable measures of magic [33]. For $\alpha \geq 2$, recent work has proved that these SRE are magic monotones thus they are good measures of magic [34]. In this work, we focus on 2-SRE, i.e., the case where $\alpha = 2$.

Suppose we have an n -qubit quantum state $|\psi\rangle$ represented by a TIMPS characterized by a tensor A^s with bond dimension χ :

$$|\psi[A^s]\rangle = \sum_{s_1, s_2, \dots, s_n} \text{tr}(A^{s_1} A^{s_2} \dots A^{s_n}) |s_1 s_2 \dots s_n\rangle, \quad (2)$$

and we define four kinds of transfer matrix E^t as shown in Fig. 2(a)

$$E^t = \sum_{s, s'=0}^1 \frac{\sigma_{s, s'}^t}{\sqrt{2}} (A^s \otimes \bar{A}^{s'}), \quad (3)$$

where t can be 0, 1, 2, 3 and $\sigma_{s, s'}^t$ is the matrix element of Pauli matrix σ^t . The \bar{A}^s is the complex conjugate of tensor A^s . Now, the quantity $\|\Xi(|\psi\rangle)\|^\alpha = \sum_{P \in \mathcal{P}_n} \Xi_P^\alpha(|\psi\rangle)$ can be directly expressed using E^t , so the SRE for TIMPS is simply

$$M_\alpha(|\psi\rangle) = \frac{1}{1-\alpha} \log \text{tr} \left[\left(\sum_{t=0}^3 (E^t)^{\otimes 2\alpha} \right)^n \right] - n \log 2. \quad (4)$$

Direct calculating $\|\Xi(|\psi\rangle)\|^\alpha$ in terms of E^t remains challenging because E^t is a $\chi^2 \times \chi^2$ matrix, and $(E^t)^{\otimes 4}$ has order χ^8 , which grows rapidly. The rapid polynomial growth in matrix dimension makes it challenging to compute the SRE for MPS numerically, even for small bond dimensions. Therefore, truncation is required to calculate the SRE more efficiently and this approach will be discussed in the following section.

Based on the expression of SRE for TIMPS (4), we are able to obtain some analytical result for quantum states that have simple MPS representation.

We first calculate the product state that has the form

$$|\psi_n(\theta, \phi)\rangle = \left(\cos \frac{\theta}{2} |0\rangle + e^{i\phi} \sin \frac{\theta}{2} |1\rangle \right)^{\otimes n} \quad (5)$$

which can be expressed in TIMPS form with bond dimension $\chi = 1$. The calculation is very easy because transfer matrices are just numbers now and it is clear from Eq. (4) that

$$M_2(|\psi_n(\theta, \phi)\rangle) = nM_2(|\psi_1(\theta, \phi)\rangle) \quad (6)$$

which is also the direct result of the requirement from resource theory, i.e.,

$$M_\alpha(|\psi\rangle \otimes |\phi\rangle) = M_\alpha(|\psi\rangle) + M_\alpha(|\phi\rangle), \quad (7)$$

and this is often called the additivity of α -SRE [22].

The calculation of $|\psi_1(\theta, \phi)\rangle$ yields

$$M_2(|\psi_1(\theta, \phi)\rangle) = -\log \left[\cos^8 \frac{\theta}{2} + \sin^8 \frac{\theta}{2} + \frac{6 + \cos 4\phi}{8} \sin^4 \theta \right] \quad (8)$$

and it reaches the maximum value $\log \frac{3}{2}$ at $(\theta_m, \phi_m) = (2 \arccos \sqrt{\frac{3-\sqrt{3}}{6}}, \frac{\pi}{4})$. We note that this is not the only maximum point. Due to the stability of SRE under Clifford operations [22], the state $|\psi_1(\theta_m, \phi_m)\rangle$ with any Clifford gate acted on reaches the maximum value of SRE.

Next, we calculate the SRE of GHZ-like state, defined as

$$|\text{GHZ}_n(\theta, \phi)\rangle = \cos \frac{\theta}{2} |0\rangle^{\otimes n} + e^{i\phi} \sin \frac{\theta}{2} |1\rangle^{\otimes n}. \quad (9)$$

This state can be expressed in TIMPS with bond dimension $\chi = 2$ so we can't use the trick from Eq. (7). However, the form of transfer matrices are very simple. They are sparse and diagonal thus making the calculation of SRE possible. The final result for state $|\text{GHZ}_n(\theta, \phi)\rangle$ is

$$M_2(|\text{GHZ}_n(\theta, \phi)\rangle) = M_2(|\psi_1(\theta, \phi)\rangle), \quad (10)$$

that is, the SRE of GHZ-like state equals to the SRE of a single qubit with the same parameters. This is not a surprising result because if we adopt the perspective of quantum circuit, the GHZ-like state can be prepared by a single-qubit rotation gate followed by many CNOT gates and we know CNOT gate is a Clifford operation so the magic can only be generated from the single-qubit rotation.

Based on the SRE of TIMPS, we can also calculate the SRE of W state which has the form of

$$|W_n\rangle = \frac{|10 \cdots 0\rangle + |01 \cdots 0\rangle + \cdots + |00 \cdots 1\rangle}{\sqrt{n}}. \quad (11)$$

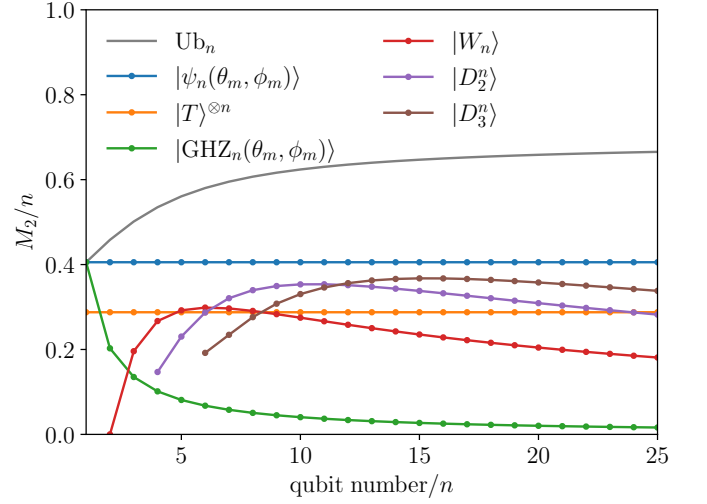


FIG. 1. The SRE density $m_2 = M_2/n$ as the function of qubit number n for different quantum states. The grey line is the theoretical upper bound of the SRE which is $\text{Ub}_n = [\log(2^n + 1) - \log 2]/n$.

The W states are genuine multipartite entangled states and it has been applied widely in quantum information theory [35]. Although the W state is translationally invariant, it does not have a simple TIMPS representation under periodic boundary condition [36, 37]. However, an MPS representation with bond dimension $\chi = 2$ for the W state can be easily obtained under open boundary conditions, where the bulk tensors are translationally invariant. Therefore, our method remains applicable. We note that the SRE of W states has been calculated previously in [38, 39] where the authors directly calculated the SRE of W state defined as $|W'_L\rangle = \frac{1}{\sqrt{L}} \sum_{i=1}^L \sigma_i^z |-\rangle^{\otimes L}$ and their result is $M_2(|W'_L\rangle) = 3 \log L - \log(7L - 6)$. The definition of $|W_n\rangle$ and $|W'_L\rangle$ differs only in the basis and this can be synchronized by Hadamard gate which is also a Clifford operation. Therefore, the two W states have the same SRE and the calculation of W state using TIMPS indeed yields the same result.

However, our method can be used to calculate more complex quantum states. The Dicke state is defined as

$$|D_k^n\rangle = \frac{1}{\sqrt{C_n^k}} \sum_i \mathcal{P}_i(|0\rangle^{\otimes n-k} \otimes |1\rangle^{\otimes k}) \quad (12)$$

where \mathcal{P}_i is the permutation operator and summation is over all distinct permutations [40]. The W state is actually a special Dicke state with $k = 1$. The Dicke state is a permutationally invariant state, therefore their SRE can be evaluated numerically in a more efficient way [41]. But the analytical expression of the Dicke state's SRE is still not easy to obtain. Here we provide the analytical expression for the SRE of $k = 2$ and $k = 3$ Dicke states through the direct calculation of transfer matrices. Our

result for $k = 2$ is

$$M_2(|D_2^n\rangle) = 3\log n(n-1) - \log(91n^2 - 427n + 492) - 2\log 2, \quad (13)$$

and for $k = 3$ we obtain

$$M_2(|D_3^n\rangle) = -\log(1645n^3 - 18921n^2 + 71708n - 89244) + 3\log n(n-1)(n-2) - 2\log 6. \quad (14)$$

where $n \geq 4$ and $n \geq 6$ for Eq. (13) and Eq. (14), respectively. We note that this is also the SRE of $|D_{n-2}^n\rangle$ (and $|D_{n-3}^n\rangle$) due to the spin flip symmetry of Dicke states.

As a summary, we show the SRE densities defined as $m_2(|\psi\rangle) = M_2(|\psi\rangle)/n$ of the states discussed above in Fig. 1. From the perspective of resource theory, all of the states we discussed in this section can be prepared by the state $|\psi_n(\theta_m, \phi_m)\rangle$ and Clifford gates only while the product of commonly used magic state $|T\rangle^{\otimes n} = |\psi_n(\pi/2, \pi/4)\rangle$ can not be used to prepare some of the W and $k = 2, 3$ Dicke states if we restrict the qubit number n is the same.

III. SRE IN INFINITE MPS

Similar to other thermodynamic quantities, the SRE is an extensive property of quantum states. Thus we study the density of SRE for a n -qubit state $|\psi\rangle$ which has been defined previously as $m_2(|\psi\rangle) = M_2(|\psi\rangle)/n$, and the upper bound of 2-SRE M_2 directly provides the upper bound of m_2 in the thermodynamic limit [22]

$$\lim_{n \rightarrow \infty} m_2(|\psi\rangle) < \lim_{n \rightarrow \infty} \frac{\log(2^n + 1) - \log 2}{n} = \log 2. \quad (15)$$

For a quantum state $|\psi\rangle$ represented by an iMPS characterized by a tensor A^s with bond dimension χ

$$|\psi[A^s]\rangle = \sum_{\dots, s_i, s_{i+1} \dots} \dots A^{s_i} A^{s_{i+1}} \dots |\dots s_i s_{i+1} \dots\rangle, \quad (16)$$

we denote D and its eigendecomposition

$$D = \sum_{t=0}^3 (E^t)^{\otimes 4} = \sum_{i=0}^{\chi^8-1} \lambda_i(D) |\lambda_i(D)\rangle \langle \lambda_i(D)|, \quad (17)$$

where $\lambda_i(D)$ is the i -th eigenvalue and we assume $\lambda_0(D) > \lambda_1(D) \geq \dots \geq \lambda_{\chi^8-1}(D)$. Now it is easy to show that the density of SRE of $|\psi\rangle$ is

$$\begin{aligned} m_2(|\psi\rangle) &= -\lim_{n \rightarrow +\infty} \frac{\log(\text{tr } D^n)}{n} - \log 2 \\ &= -\lim_{n \rightarrow +\infty} \frac{1}{n} \log \sum_i \lambda_i(D)^n - \log 2 \\ &= -\log \lambda_0(D) - \log 2, \end{aligned} \quad (18)$$

which indicates that the SRE density of iMPS, unlike entanglement, can be solely determined by the property

of local tensor A^s . This result has been previously shown in [25, 42, 43].

Due to the prohibitively large bond dimension of D , it is essential to efficiently reduce the bond dimensions of both E^t and $(E^t)^{\otimes 2}$ prior to computing the dominant eigenvalue of D . A natural strategy to achieve this is to adopt the Pauli-MPS method proposed in [26], adapted to the iMPS setting. The core steps of this adapted method are outlined in Algorithm 1, and we refer to this modified approach as the Pauli-iMPS method. However, we observe that the Pauli-iMPS method shows numerical instabilities near the critical point, as shown in Fig. 3(a). To address this issue, we develop a new algorithm called bond-DMRG. The basic idea of this new algorithm is to construct the matrix product operator (MPO) representation of matrix D and use the standard density matrix renormalization group (DMRG) technique [44, 45] to obtain the dominant eigenvalue $\lambda_0(D)$ and thus the SRE density can be directly calculated. The detailed construction procedures of MPO of matrix D are shown in [46].

Algorithm 1 Pauli iMPS algorithm

Require: local tensor of an iMPS A^s , cutoffs ϵ_1, ϵ_2

- 1: turn A^s into left canonical form $A^s \rightarrow \{A_L^s, C\}$
 - 2: calculate E_L^t using Eq. (3), and let $E_C = C \otimes \bar{C}$
 - 3: perform SVD and truncate singular values smaller than ϵ_1 such that $E_C \approx U_{\chi^2 \times d} S_{d \times d} V_{d \times \chi}^\dagger$
 - 4: $\tilde{E}_L^t \leftarrow U^\dagger E_L^t U$, $\tilde{E}_C \leftarrow S_{d \times d}$ $\triangleright d \leq \chi^2$
 - 5: $\tilde{G}_L^t \leftarrow \sum_{t_1, t_2} \delta_{t_1, t_2}^t (\tilde{E}_L^{t_1} \otimes \tilde{E}_L^{t_2})$, $\tilde{G}_C \leftarrow \tilde{E}_C^{\otimes 2}$
 - 6: perform SVD and truncate singular values smaller than ϵ_2 such that $\tilde{G}_C \approx U_{d^2 \times m} S_{m \times m} V_{m \times d^2}^\dagger$
 - 7: $\tilde{G}_L^t \leftarrow U^\dagger \tilde{G}_L^t U$, $\tilde{G}_C \leftarrow S_{m \times m}$ $\triangleright m \leq d^2 \leq \chi^4$
 - 8: $D_L \leftarrow \sum_t \tilde{G}_L^t \otimes \tilde{G}_L^t$
 - 9: calculate the dominant eigenvalue of D_L and the SRE density is obtained
-

For comparison, we employ both of the aforementioned numerical methods to compute the SRE density of ground states in quantum Ising model directly in the thermodynamic limit. This is achieved using VUMPS algorithm [47, 48], applied to the Hamiltonian

$$\hat{H} = -h_x \sum_i \hat{\sigma}_i^x - J \sum_i \hat{\sigma}_i^z \hat{\sigma}_{i+1}^z, \quad (19)$$

where $J = 1$ is fixed. As a baseline for comparison, we also compute the SRE density in a finite system of size $L = 128$ using the Pauli-MPS method. The results are presented in Fig. 3(a), where the Pauli-iMPS method exhibits numerical instabilities in the vicinity of the critical point. In particular, for $h_x/J \geq 1$, the computed values deviate noticeably from the expected results. In contrast, the bond-DMRG method demonstrates robust numerical stability across the entire parameter regime. Remarkably, even with a modest bond dimension of $\chi = 8$, the SRE density obtained via bond-DMRG remains in excellent agreement with the baseline results.

Building on the observed stability and accuracy of the bond-DMRG method, we further investigate the relation-

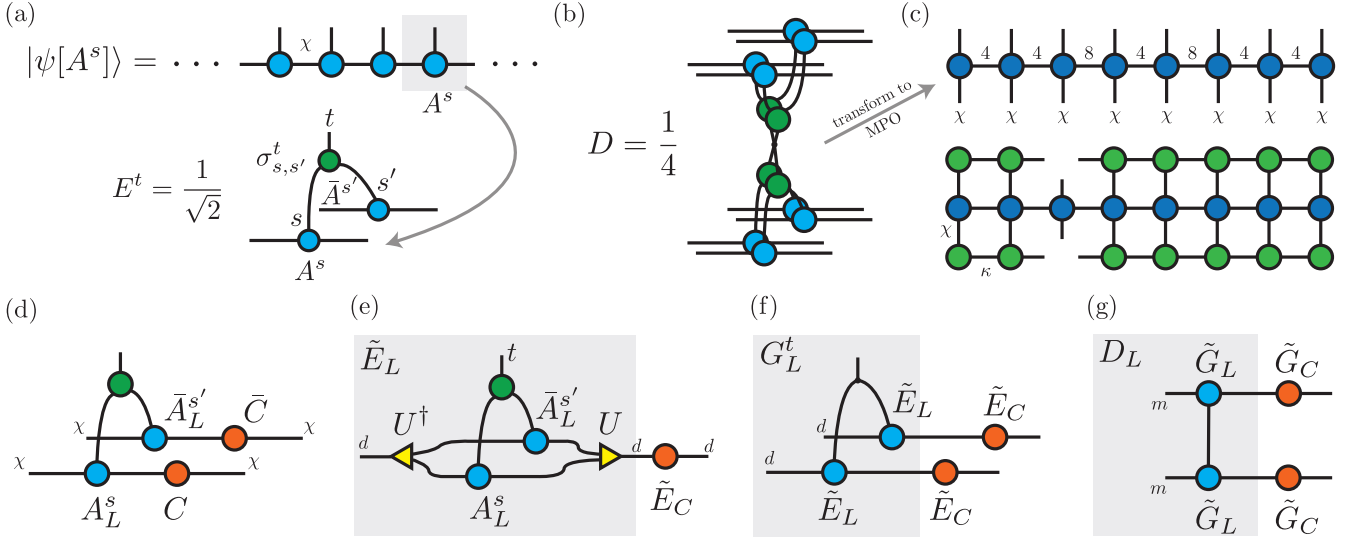


FIG. 2. (a) and (b) show how tensors are contracted in Eq. (3) and Eq. (17) respectively. (c) The basic idea of bond-DMRG algorithm is to construct the MPO form of matrix D and perform standard DMRG to obtain the dominant eigenvalue. The bond dimension of matrix D 's MPO is no more than 8 thus making bond-DMRG very efficient when χ is not too large. (d-g) show how tensors are contracted in Algorithm 1.

ship between SRE density and entanglement in iMPS characterized by random tensors of the form $(A^s)_{ij} = r_{ij}^s e^{i2\pi\theta_{ij}^s}$, where r_{ij}^s and θ_{ij}^s are independent random variables uniformly distributed in the interval $[0, 1]$. Prior to computing relevant physical quantities, local tensor A^s has to be normalized according to the transformation $A^s \rightarrow A^s / \sqrt{\lambda_0(E^0)}$ where $\lambda_0(E^0)$ denotes the dominant eigenvalue of the transfer matrix E^0 defined in Eq. (3).

The distribution of the SRE density m_2 for random iMPS is presented in Fig. 3(b). As illustrated in the inset, the average value of m_2 increases with the bond dimension χ . This finding suggests two notable observations. First, weakly entangled quantum states can still exhibit relatively high SRE density. In particular, for $\chi = 5$, the majority of random iMPS approach the theoretical upper bound of m_2 , indicating that significant SRE can emerge even in moderately entangled systems. Second, the distributions for different values of χ appear to converge toward a universal shape as χ increases. Determining the limiting form of this distribution in the $\chi \rightarrow \infty$ limit presents an interesting direction for future research. During the course of these calculations, we observed that for random iMPS, convergence of the SRE density requires the bond dimension κ of the bond-DMRG states to scale approximately as $\kappa \sim \chi^4/2$. Consequently, computational constraints limit our study to bond dimensions up to $\chi = 5$. For instance, at $\chi = 6$, the required bond dimension reaches $\kappa = 648$, making the sampling process prohibitively time-consuming.

We now investigate the relationship between the SRE density m_2 and the entanglement spectrum $\{p_i = \lambda_i^2\}$ in random iMPS, for which both quantities can now be

efficiently computed. To characterize the entanglement spectrum, we focus on two key properties. The first is the entanglement entropy, defined as $S = -\sum_i p_i \log p_i$. The second property is the (anti-)flatness of the entanglement spectrum, as introduced in [23]. Consider a pure state $|\psi\rangle$ in a bipartite system $\mathcal{H} = \mathcal{H}_A \otimes \mathcal{H}_B$, with reduced density matrix $\rho_A = \text{tr}_B |\psi\rangle\langle\psi|$. The (anti-)flatness is defined by $\mathcal{F}_A(|\psi\rangle) := \text{tr}(\rho_A^3) - [\text{tr}(\rho_A^2)]^2$, which captures the deviation of the entanglement spectrum from uniformity. In Ref. [23], it was further demonstrated that the flatness is related to the stabilizer linear entropy M_{lin} . However, the stabilizer linear entropy is not well-defined in the thermodynamic limit. Specifically, one finds that its density $m_{\text{lin}} = 0$ in the thermodynamic limit for all states. Therefore, we still focus on m_2 and study its relation with not flatness but “logarithmic (anti-)flatness” first introduced in [49], which is defined as

$$F(\rho) := \log[\text{tr}(\rho^3)] - \log[\text{tr}(\rho^2)]^2. \quad (20)$$

It is evident that for product states, the flatness (and logarithmic flatness) vanishes, yet such states may still possess non-stabilizerness. To capture the component of SRE that cannot be eliminated by local unitary transformations, we define the non-local SRE density for a n -qubit state as

$$\tilde{m}_2(|\psi\rangle) = \min_{\{U_i\}} m_2 \left[\left(\bigotimes_{i=1}^n U_i \right) |\psi\rangle \right], \quad (21)$$

where the minimization is performed over all single-site unitary operations $U_i \in \text{SU}(2)$. In finite systems, evaluating \tilde{m}_2 is computationally challenging, as the optimal local unitary can, in general, vary from site to site. However, for translationally invariant iMPS, this difficulty

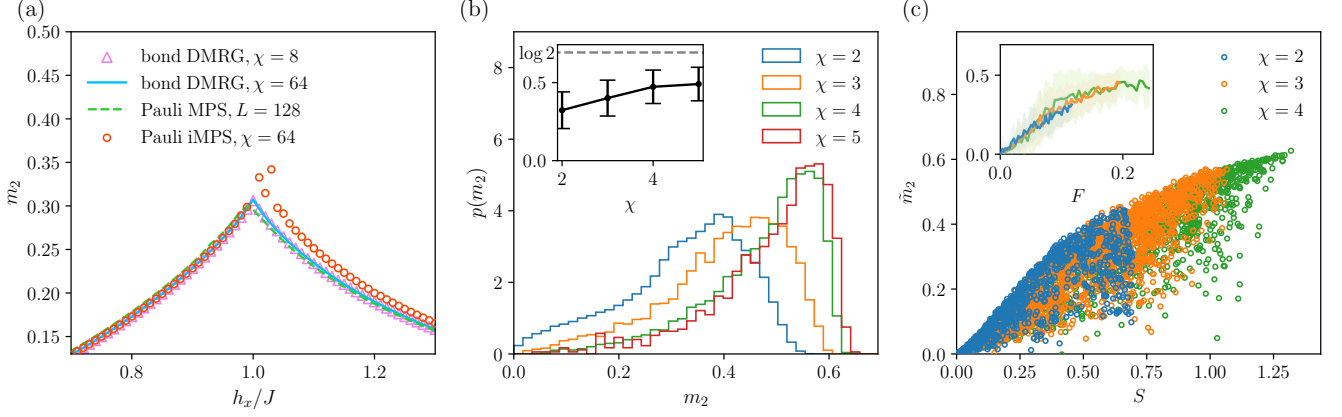


FIG. 3. (a) The SRE densities calculated using the bond-DMRG and Pauli-iMPS methods for the infinite system, as well as the Pauli-MPS method for a finite system of size $L = 128$. The Pauli-iMPS results exhibit numerical instabilities near the critical point, and the values for $h_x/J \geq 1$ deviate from the correct ones. In contrast, the bond-DMRG method demonstrates good stability across. (b) The distributions of the SRE density m_2 for random iMPS. Inset: the average value of m_2 increases with the bond dimension χ , highlighting the growing capacity for non-stabilizerness in more entangled states. (c) The sampled data. The non-local SRE density \tilde{m}_2 appears to be bounded by a universal function of the entanglement entropy, i.e., $\tilde{m}_2 \leq f(S)$, independently of the bond dimension χ . Inset: the relationship between \tilde{m}_2 and the logarithmic flatness F .

is mitigated: the optimal local unitary minimizing m_2 must be the same at every site. This symmetry greatly simplifies the minimization procedure and allows us to systematically explore the behavior of \tilde{m}_2 for iMPS with small bond dimensions.

We perform numerical evaluations of \tilde{m}_2 across ensembles of random iMPS to investigate its dependence on the entanglement structure. As shown in Fig. 3(c), the non-local SRE density \tilde{m}_2 are observed to be upper bounded by a function of the entanglement entropy S , i.e., $\tilde{m}_2 \leq f(S)$, where the function f appears to be independent of the bond dimension χ . This finding implies there is a universal constraint on the maximal amount of non-local non-stabilizerness that a state can support for a given level of entanglement entropy. Moreover, the inset of Fig. 3(c) shows the relationship between \tilde{m}_2 and the logarithmic flatness F of the entanglement spectrum. A positive statistical correlation is clearly observed: states with larger F tend to exhibit larger values of \tilde{m}_2 . This suggests that logarithmic flatness can serve as a useful indicator of non-local non-stabilizer resource. Taken together, these observations demonstrate that both the total and non-local SRE densities are closely governed by the entanglement structure of the state, with \tilde{m}_2 providing a finer-grained characterization of non-stabilizerness that is robust under local basis transformations.

IV. MUTUAL SRE FOR TIMPS

Similar to quantum mutual information, the mutual SRE, as a measure of long-range magic, can be defined for quantum many-body systems. First, we introduce the

2-SRE definition for a n -qubit mixed state ρ

$$\tilde{M}_2(\rho) := M_2(\rho) - S_2(\rho), \quad (22)$$

where $M_2(\rho) = -\log \sum_{P \in \mathcal{P}_n} \text{tr}(P\rho)^4$ is the generalization of Eq. (1) and $S_2(\rho) = -\log \text{tr}(\rho^2)$ is the Rényi-2 entropy [22]. The 2-SRE for mixed state ρ can be seen as the Rényi-2 entropy of $\tilde{\Xi}_P = |\text{tr}(P\rho)^2| / \sum_{P \in \mathcal{P}_n} |\text{tr}(P\rho)|^2$ apart from some offset and the free states are defined as the mixed states that can be obtained from pure stabilizer states by partial tracing [22, 27].

We can now define a measure of long-range magic, called mutual SRE (mSRE), analogous to mutual information, and denote it as $L(\rho_{AB})$:

$$L(\rho_{AB}) = \tilde{M}_2(\rho_{AB}) - \tilde{M}_2(\rho_A) - \tilde{M}_2(\rho_B), \quad (23)$$

where A and B are two separated subsystems. This mSRE measures the extent to which magic is encoded in the correlations between subsystems, thereby quantifying the degree to which magic cannot be eliminated by finite-depth quantum circuits [27, 50].

We focus on the mSRE between two different sites in an iMPS. For an iMPS characterized by a tensor A^s , we consider two subsystems A and B separated by a distance r , where $s_2 - s_1 - 1 = r$ with s_1 and s_2 representing the sites of subsystems A and B , respectively. Due to the translational invariance of iMPS, the mSRE $L(\rho_{AB})$ between A and B only depends on their distance r .

The mSRE consists of two parts $L(\rho_{AB}) = L_M(\rho_{AB}) + L_S(\rho_{AB})$ where $L_M(\rho_{AB}) = M_2(\rho_{AB}) - 2M_2(\rho_A)$ and $L_S(\rho_{AB}) = 2S_2(\rho_A) - S_2(\rho_{AB})$. The $L_S(\rho_{AB})$ is actually the mutual information defined with Rényi-2 entropy. Denoting a new transfer matrix and its eigendecompo-

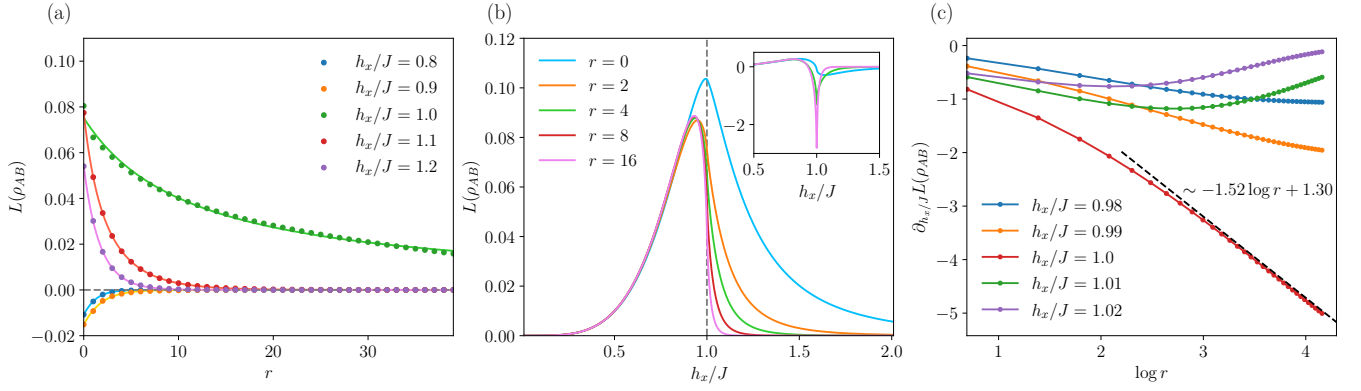


FIG. 4. (a) The two-point mSRE in the ground state of the quantum Ising model. The colored dots represent the results from DMRG, while the lines are obtained from the fitting results. (b) The exact mSRE $L(\rho_{AB})$ for the Ising model with unbroken \mathbb{Z}_2 symmetry shows a non-vanishing behaviour in the ferromagnetic phase and vanishing one in the paramagnetic phase. Inset: the derivative of $L(\rho_{AB})$ exhibits a sharp peak at the critical point as the distance between two subsystems increases. (c) We calculate the derivative of $L(\rho_{AB})$ for the Ising model with unbroken \mathbb{Z}_2 symmetry near the critical point and observe that its value at the critical point follows a logarithmic scaling behavior, as described in Eq. (29).

sition

$$E_A^{\bar{A}} = \sqrt{2}E^0 = \sum_{s=0}^1 A^s \otimes \bar{A}^s = |r\rangle(l| + \sum_i \lambda_i |\lambda_i\rangle\langle\lambda_i|), \quad (24)$$

where the vectors $|l\rangle$ and $|r\rangle$ satisfy $(l|E_A^{\bar{A}} = (l|$ and $E_A^{\bar{A}}|r\rangle = |r\rangle$, we can directly obtain the expression for ρ_A, ρ_B and ρ_{AB}

$$\rho_A = (l|(A^{s_1} \otimes \bar{A}^{s'_1})|r\rangle), \quad (25)$$

$$\rho_B = (l|(A^{s_2} \otimes \bar{A}^{s'_2})|r\rangle), \quad (26)$$

$$\begin{aligned} \rho_{AB} &= (l|(A^{s_1} \otimes \bar{A}^{s'_1})(E_A^{\bar{A}})^r(A^{s_2} \otimes \bar{A}^{s'_2})|r\rangle) \\ &= \rho_A \otimes \rho_B + \sum_i \lambda_i^r \rho_l(\lambda_i) \otimes \rho_r(\lambda_i), \end{aligned} \quad (27)$$

where $\rho_l(\lambda_i) = (l|(A^{s_1} \otimes \bar{A}^{s'_1})|\lambda_i\rangle)$ and $\rho_r(\lambda_i) = (\lambda_i|(A^{s_2} \otimes \bar{A}^{s'_2})|r\rangle)$. By substituting the expressions of ρ_A, ρ_B and ρ_{AB} in Eq. (23), we obtain the long-range limit ($r \rightarrow +\infty$) for mSRE

$$\lim_{r \rightarrow +\infty} L(\rho_{AB}) = \lim_{r \rightarrow +\infty} \log \left[\frac{1 + 2\lambda_1^r c_s}{1 + 2\lambda_1^r c_m} \right] = 0, \quad (28)$$

where $|\lambda_1| \in [0, 1)$ is the second largest eigenvalue of transfer matrix $E_A^{\bar{A}}$ and c_s, c_m are constants independent of distance r . The explicit expressions of c_s and c_m can be

TABLE I. The fitted values of the parameters c_s, c_m and λ_1 are shown below and the curves are shown in Fig. 4 (a).

h_x/J	0.8	0.9	1.0	1.1	1.2
c_s	0.151	0.049	-0.499	-0.218	-0.047
c_m	0.158	0.057	-0.499	-0.239	-0.071
λ_1	0.397	0.561	0.999	0.764	0.583

found in [46]. Therefore, we prove that for any injective iMPS, e.g., ground states of gapped systems, the two-point mSRE will eventually decay to zero as the distance r tends to infinity and the long-range behaviour of mSRE takes the form of $L(\rho_{AB}) \sim \log \frac{1+2\lambda_1^r c_s}{1+2\lambda_1^r c_m}$.

Next, to calculate the two-point mSRE in the ground state of quantum Ising model, we perform DMRG [44, 45] calculation in a chain of size $L = 128$ and extract the mSRE between the middle site $s_1 = 64$ and $s_2 = s_1 + r + 1$ with $r \in [0, 39]$. The numerical results are shown in Fig. 4(a) where we also use the asymptotic behavior of $L(\rho_{AB})$ to extract the c_s, c_m and λ_1 . We note that the λ_1 is directly related to the correlation length of the system [48, 51], $\xi = -1/\ln|\lambda_1|$. We also show the fitting parameters c_s, c_m and λ_1 in Table I. It can be found that near the critical point $h_x/J = 1$, λ_1 approaches 1 thus indicating the divergence of correlation length at $h_x/J = 1$.

In addition to the decay behavior of the two-point mSRE, the analytical calculation of the mSRE for the Ising model without symmetry breaking reveals a clear distinction: in the ferromagnetic phase, the mSRE remains finite, whereas in the paramagnetic phase, it vanishes, as shown in Fig. 4(b). This behavior can be attributed to the modified asymptotic form of $L(\rho_{AB}) \sim \log \frac{1+2\lambda_1^r c_s}{1+2\lambda_1^r c_m} + \log c$ where the parameter c arises due to the unbroken symmetry. In Fig. 4(b), we also observe that the mSRE does not attain its maximum at the critical point. Instead, it reaches its peak slightly before $h_x/J = 1$ for all values of r . However, the derivative of the mSRE exhibits a pronounced peak at the critical point, which becomes increasingly sharp with larger r , following a scaling behavior of

$$\left. \frac{\partial L(\rho_{AB})}{\partial (h_x/J)} \right|_{h_x/J=1} \sim \log r, \quad (29)$$

as observed in Fig. 4(c). These observations lead to two conclusions. First, long-range entanglement appears to be a necessary condition for the emergence of long-range mSRE. Second, the derivative of the long-range mSRE may serve as a robust indicator of quantum phase transitions.

V. DISCUSSION AND OUTLOOK

We study stabilizer Rényi entropy in translationally invariant matrix product states. Analytical results are first derived for representative quantum states and then we develop an efficient algorithm to compute the SRE density in iMPS and apply it to the one-dimensional Ising model, where the SRE density peaks and exhibits non-analytic behavior at the critical point. Using this algorithm, we analyze the (non-local) SRE in random iMPS ensembles. We find it is bounded by a universal function of entanglement entropy and positively correlated with the logarithmic flatness of the entanglement spectrum. Finally, we study the asymptotic behavior of mSRE, which also displays non-analyticity near criticality, highlighting a potential link between mSRE and quantum phase transitions.

Several open questions remain for future investigation. First, deriving general expressions for the SRE of Dicke states with $k \geq 4$ is challenging, as brute-force methods

become infeasible due to rapidly growing bond dimensions. Notably, the maximal SRE density appears to increase with k , prompting the question of whether it can surpass the single-qubit bound $\log \frac{3}{2}$. It is also of interest to determine the limiting form of the SRE density distribution of random iMPS as $\chi \rightarrow \infty$, and to identify the explicit form of the universal function bounding the non-local SRE. Furthermore, obtaining analytical expressions for the SRE and mSRE in the Ising model, particularly near the critical point using conformal field theory (CFT) techniques, would be highly valuable. In this context, recent progress has been made in relating SRE to CFT frameworks [52]. Finally, investigating the connections between mSRE and other emerging measures of magic, such as non-stabilizer entanglement entropy [53] and quantum non-local magic [54], may provide deeper insights into the structure of non-stabilizerness in quantum many-body systems.

ACKNOWLEDGMENTS

This work is supported by the National Key Research and Development of China (Grant Nos. 2021YFA1402001, 2021YFA0718304) and the National Natural Science Foundation of China (NSFC) (Grant Nos. 12375007, 12135018).

-
- [1] R. Horodecki, P. Horodecki, M. Horodecki, and K. Horodecki, Quantum entanglement, *Rev. Mod. Phys.* **81**, 865 (2009).
 - [2] T. J. Osborne and M. A. Nielsen, Entanglement in a simple quantum phase transition, *Phys. Rev. A* **66**, 032110 (2002).
 - [3] V. Vedral, High-temperature macroscopic entanglement, *New Journal of Physics* **6**, 102 (2004).
 - [4] D. A. Abanin, E. Altman, I. Bloch, and M. Serbyn, Colloquium: Many-body localization, thermalization, and entanglement, *Rev. Mod. Phys.* **91**, 021001 (2019).
 - [5] N. Tantivasadakarn, R. Thorngren, A. Vishwanath, and R. Verresen, Long-range entanglement from measuring symmetry-protected topological phases, *Phys. Rev. X* **14**, 021040 (2024).
 - [6] X. Chen, Z.-C. Gu, and X.-G. Wen, Local unitary transformation, long-range quantum entanglement, wave function renormalization, and topological order, *Phys. Rev. B* **82**, 155138 (2010).
 - [7] X.-G. Wen, Choreographed entanglement dances: Topological states of quantum matter, *Science* **363**, eaal3099 (2019).
 - [8] C. Broholm, R. J. Cava, S. A. Kivelson, D. G. Nocera, M. R. Norman, and T. Senthil, Quantum spin liquids, *Science* **367**, eaay0668 (2020).
 - [9] C. H. Bennett, Quantum information, *Physica Scripta* **1998**, 210 (1998).
 - [10] R. Jozsa, Entanglement and quantum computation (1997), [arXiv:quant-ph/9707034 \[quant-ph\]](#).
 - [11] D. Gottesman, [An introduction to quantum error correction and fault-tolerant quantum computation](#) (2009), [arXiv:0904.2557 \[quant-ph\]](#).
 - [12] G. Vidal, Efficient classical simulation of slightly entangled quantum computations, *Physical Review Letters* **91**, 10.1103/physrevlett.91.147902 (2003).
 - [13] U. Schollwöck, The density-matrix renormalization group in the age of matrix product states, *Annals of Physics* **326**, 96–192 (2011).
 - [14] D. Gottesman, [The heisenberg representation of quantum computers](#) (1998), [arXiv:quant-ph/9807006 \[quant-ph\]](#).
 - [15] V. Veitch, S. A. Hamed Mousavian, D. Gottesman, and J. Emerson, The resource theory of stabilizer quantum computation, *New Journal of Physics* **16**, 013009 (2014).
 - [16] S. Bravyi, G. Smith, and J. A. Smolin, Trading classical and quantum computational resources, *Phys. Rev. X* **6**, 021043 (2016).
 - [17] S. Bravyi, D. Browne, P. Calpin, E. Campbell, D. Gosset, and M. Howard, Simulation of quantum circuits by low-rank stabilizer decompositions, *Quantum* **3**, 181 (2019).
 - [18] S. Bravyi and D. Gosset, Improved classical simulation of quantum circuits dominated by clifford gates, *Phys. Rev. Lett.* **116**, 250501 (2016).
 - [19] H. Pashayan, J. J. Wallman, and S. D. Bartlett, Estimating outcome probabilities of quantum circuits using quasiprobabilities, *Phys. Rev. Lett.* **115**, 070501 (2015).
 - [20] M. Howard and E. Campbell, Application of a resource theory for magic states to fault-tolerant quantum com-

- puting, *Phys. Rev. Lett.* **118**, 090501 (2017).
- [21] Z.-W. Liu and A. Winter, Many-body quantum magic, *PRX Quantum* **3**, 020333 (2022).
 - [22] L. Leone, S. F. E. Oliviero, and A. Hamma, Stabilizer rényi entropy, *Phys. Rev. Lett.* **128**, 050402 (2022).
 - [23] E. Tirrito, P. S. Tarabunga, G. Lami, T. Chanda, L. Leone, S. F. E. Oliviero, M. Dalmonte, M. Collura, and A. Hamma, Quantifying nonstabilizerness through entanglement spectrum flatness, *Phys. Rev. A* **109**, L040401 (2024).
 - [24] A. Gu, S. F. Oliviero, and L. Leone, Magic-induced computational separation in entanglement theory, *PRX Quantum* **6**, 020324 (2025).
 - [25] T. Haug and L. Piroli, Quantifying nonstabilizerness of matrix product states, *Phys. Rev. B* **107**, 035148 (2023).
 - [26] P. S. Tarabunga, E. Tirrito, M. C. Bañuls, and M. Dalmonte, Nonstabilizerness via matrix product states in the pauli basis, *Phys. Rev. Lett.* **133**, 010601 (2024).
 - [27] P. S. Tarabunga, E. Tirrito, T. Chanda, and M. Dalmonte, Many-body magic via pauli-markov chains—from criticality to gauge theories, *PRX Quantum* **4**, 040317 (2023).
 - [28] A. Cabello, Bell’s theorem with and without inequalities for the three-qubit greenberger-horne-zeilinger and w states, *Phys. Rev. A* **65**, 032108 (2002).
 - [29] M. Hillery, V. Bužek, and A. Berthiaume, Quantum secret sharing, *Phys. Rev. A* **59**, 1829 (1999).
 - [30] M. Fleischhauer and M. D. Lukin, Quantum memory for photons: Dark-state polaritons, *Phys. Rev. A* **65**, 022314 (2002).
 - [31] R. Prevedel, G. Cronenberg, M. S. Tame, M. Paternostro, P. Walther, M. S. Kim, and A. Zeilinger, Experimental realization of dicke states of up to six qubits for multiparty quantum networking, *Phys. Rev. Lett.* **103**, 020503 (2009).
 - [32] A. Bärttschi and S. Eidenbenz, Deterministic preparation of dicke states, in *Fundamentals of Computation Theory* (Springer International Publishing, 2019) p. 126–139.
 - [33] T. Haug and L. Piroli, Stabilizer entropies and nonstabilizerness monotones, *Quantum* **7**, 1092 (2023).
 - [34] L. Leone and L. Bittel, Stabilizer entropies are monotones for magic-state resource theory, *Phys. Rev. A* **110**, L040403 (2024).
 - [35] W. Dür, G. Vidal, and J. I. Cirac, Three qubits can be entangled in two inequivalent ways, *Phys. Rev. A* **62**, 062314 (2000).
 - [36] D. Perez-Garcia, F. Verstraete, M. M. Wolf, and J. I. Cirac, Matrix product state representations (2007), [arXiv:quant-ph/0608197](https://arxiv.org/abs/quant-ph/0608197) [quant-ph].
 - [37] P. Klimov, R. Sengupta, and J. Biamonte, On translation-invariant matrix product states and advances in mps representations of the w -state (2023), [arXiv:2306.16456](https://arxiv.org/abs/2306.16456) [quant-ph].
 - [38] J. Odavić, T. Haug, G. Torre, A. Hamma, F. Franchini, and S. M. Giampaolo, Complexity of frustration: A new source of non-local non-stabilizerness, *SciPost Phys.* **15**, 131 (2023).
 - [39] A. G. Catalano, J. Odavić, G. Torre, A. Hamma, F. Franchini, and S. M. Giampaolo, Magic phase transition and non-local complexity in generalized w state (2025), [arXiv:2406.19457](https://arxiv.org/abs/2406.19457) [quant-ph].
 - [40] R. H. Dicke, Coherence in spontaneous radiation processes, *Phys. Rev.* **93**, 99 (1954).
 - [41] G. Passarelli, R. Fazio, and P. Lucignano, Nonstabilizerness of permutationally invariant systems, *Phys. Rev. A* **110**, 022436 (2024).
 - [42] R. Smith, Z. Papić, and A. Hallam, Non-stabilizerness in kinetically-constrained rydberg atom arrays (2024), [arXiv:2406.14348](https://arxiv.org/abs/2406.14348) [quant-ph].
 - [43] D. A. Korbany, M. J. Gullans, and L. Piroli, Long-range nonstabilizerness and phases of matter (2025), [arXiv:2502.19504](https://arxiv.org/abs/2502.19504) [quant-ph].
 - [44] S. R. White, Density matrix formulation for quantum renormalization groups, *Phys. Rev. Lett.* **69**, 2863 (1992).
 - [45] M. Fishman, S. R. White, and E. M. Stoudenmire, The ITensor Software Library for Tensor Network Calculations, *SciPost Phys. Codebases*, 4 (2022).
 - [46] See Appendices for details.
 - [47] V. Zauner-Stauber, L. Vanderstraeten, M. T. Fishman, F. Verstraete, and J. Haegeman, Variational optimization algorithms for uniform matrix product states, *Phys. Rev. B* **97**, 045145 (2018).
 - [48] L. Vanderstraeten, J. Haegeman, and F. Verstraete, Tangent-space methods for uniform matrix product states, *SciPost Phys. Lect. Notes*, 7 (2019).
 - [49] J. Odavić, M. Viscardi, and A. Hamma, Stabilizer entropy in non-integrable quantum evolutions (2025), [arXiv:2412.10228](https://arxiv.org/abs/2412.10228) [quant-ph].
 - [50] C. D. White, C. Cao, and B. Swingle, Conformal field theories are magical, *Phys. Rev. B* **103**, 075145 (2021).
 - [51] V. Zauner, D. Draxler, L. Vanderstraeten, M. Degroote, J. Haegeman, M. M. Rams, V. Stojevic, N. Schuch, and F. Verstraete, Transfer matrices and excitations with matrix product states, *New Journal of Physics* **17**, 053002 (2015).
 - [52] M. Hoshino, M. Oshikawa, and Y. Ashida, Stabilizer rényi entropy and conformal field theory (2025), [arXiv:2503.13599](https://arxiv.org/abs/2503.13599) [quant-ph].
 - [53] J. Huang, X. Qian, and M. Qin, Non-stabilizerness entanglement entropy: a measure of hardness in the classical simulation of quantum many-body systems (2024), [arXiv:2409.16895](https://arxiv.org/abs/2409.16895) [quant-ph].
 - [54] D. Qian and J. Wang, Quantum nonlocal nonstabilizerness, *Phys. Rev. A* **111**, 052443 (2025).
 - [55] G. B. Mbeng, A. Russomanno, and G. E. Santoro, The quantum Ising chain for beginners, *SciPost Phys. Lect. Notes*, 82 (2024).

Appendix A: SRE Calculation of GHZ-like, W and Dicke states

1. GHZ-like state

The GHZ-like state, defined as

$$|\text{GHZ}_n(\theta, \phi)\rangle = \cos \frac{\theta}{2} |0\rangle^{\otimes n} + e^{i\phi} \sin \frac{\theta}{2} |1\rangle^{\otimes n}, \quad (\text{A1})$$

with $\theta \in [0, \pi]$ and $\phi \in [0, 2\pi)$, can be expressed as a simple MPS with bond dimension $\chi = 2$. The site tensor A^s for GHZ-like state is

$$A^0 = \begin{pmatrix} \sqrt[n]{\cos \frac{\theta}{2}} & 0 \\ 0 & 0 \end{pmatrix}, A^1 = \begin{pmatrix} 0 & 0 \\ 0 & e^{i\phi/n} \sqrt[n]{\sin \frac{\theta}{2}} \end{pmatrix}. \quad (\text{A2})$$

For TIMPS, we can calculate its SRE only using its local tensor. Here we can easily calculate the E^t tensor for $|\text{GHZ}_n(\theta, \phi)\rangle$ state

$$E^0 = \begin{pmatrix} aa^* & 0 & 0 & 0 \\ 0 & 0 & 0 & 0 \\ 0 & 0 & 0 & 0 \\ 0 & 0 & 0 & bb^* \end{pmatrix}, E^1 = \begin{pmatrix} 0 & 0 & 0 & 0 \\ 0 & ab^* & 0 & 0 \\ 0 & 0 & a^*b & 0 \\ 0 & 0 & 0 & 0 \end{pmatrix}, E^2 = \begin{pmatrix} 0 & 0 & 0 & 0 \\ 0 & -iab^* & 0 & 0 \\ 0 & 0 & ia^*b & 0 \\ 0 & 0 & 0 & 0 \end{pmatrix}, E^3 = \begin{pmatrix} aa^* & 0 & 0 & 0 \\ 0 & 0 & 0 & 0 \\ 0 & 0 & 0 & 0 \\ 0 & 0 & 0 & -bb^* \end{pmatrix}, \quad (\text{A3})$$

where

$$a = \frac{1}{\sqrt{2}} \sqrt[n]{\cos \frac{\theta}{2}}, \quad (\text{A4})$$

$$b = \frac{e^{i\phi/n}}{\sqrt{2}} \sqrt[n]{\sin \frac{\theta}{2}}. \quad (\text{A5})$$

It is clear that all E^t matrices are in diagonal form. Thus the following calculation is rather easy using Mathematica which directly gives the SRE of the above state:

$$M_2(|\text{GHZ}_n(\theta, \phi)\rangle) = -\log \text{tr}[(E^0 \otimes^4 + E^1 \otimes^4 + E^2 \otimes^4 + E^3 \otimes^4)^n] - n \log 2 \quad (\text{A6})$$

$$= -\log \left[\cos^8 \frac{\theta}{2} + \sin^8 \frac{\theta}{2} + \frac{6 + \cos 4\phi}{8} \sin^4 \theta \right] \quad (\text{A7})$$

which is equal to the expression of single qubit SRE.

2. W state

The W state is defined as

$$|W_n\rangle = \frac{|100 \dots 0\rangle + |010 \dots 0\rangle + |001 \dots 0\rangle + \dots + |000 \dots 1\rangle}{\sqrt{n}}. \quad (\text{A8})$$

The SRE of n -qubit W state has been calculated previously in [38], the result is

$$M_2(|W_n\rangle) = 3 \log n - \log(7n - 6). \quad (\text{A9})$$

The previous paper directly calculated this result. Using TIMPS we can also obtain this result.

The MPS local tensor of W state is

$$L^0 = \begin{pmatrix} 1 & 0 \end{pmatrix}, L^1 = \begin{pmatrix} 0 & \frac{1}{\sqrt{n}} \end{pmatrix}, \quad (\text{A10})$$

$$A^0 = \begin{pmatrix} 1 & 0 \\ 0 & 1 \end{pmatrix}, A^1 = \begin{pmatrix} 0 & \frac{1}{\sqrt{n}} \\ 0 & 0 \end{pmatrix}, \quad (\text{A11})$$

$$R^0 = \begin{pmatrix} 0 \\ 1 \end{pmatrix}, R^1 = \begin{pmatrix} \frac{1}{\sqrt{n}} \\ 0 \end{pmatrix}, \quad (\text{A12})$$

and the E tensors are

$$E_L^0 = \frac{1}{\sqrt{2}} \begin{pmatrix} 1 & 0 & 0 & \frac{1}{n} \end{pmatrix}, E_L^1 = \frac{1}{\sqrt{2}} \begin{pmatrix} 0 & \frac{1}{\sqrt{n}} & \frac{1}{\sqrt{n}} & 0 \end{pmatrix}, E_L^2 = \frac{1}{\sqrt{2}} \begin{pmatrix} 0 & -i\frac{1}{\sqrt{n}} & i\frac{1}{\sqrt{n}} & 0 \end{pmatrix}, E_L^3 = \frac{1}{\sqrt{2}} \begin{pmatrix} 1 & 0 & 0 & -\frac{1}{n} \end{pmatrix}, \quad (\text{A13})$$

$$E^0 = \frac{1}{\sqrt{2}} \begin{pmatrix} 1 & 0 & 0 & \frac{1}{n} \\ 0 & 1 & 0 & 0 \\ 0 & 0 & 1 & 0 \\ 0 & 0 & 0 & 1 \end{pmatrix}, E^1 = \frac{1}{\sqrt{2}} \begin{pmatrix} 0 & \frac{1}{\sqrt{n}} & \frac{1}{\sqrt{n}} & 0 \\ 0 & 0 & 0 & \frac{1}{\sqrt{n}} \\ 0 & 0 & 0 & \frac{1}{\sqrt{n}} \\ 0 & 0 & 0 & 0 \end{pmatrix}, E^2 = \frac{1}{\sqrt{2}} \begin{pmatrix} 0 & \frac{-i}{\sqrt{n}} & \frac{-i}{\sqrt{n}} & 0 \\ 0 & 0 & 0 & \frac{-i}{\sqrt{n}} \\ 0 & 0 & 0 & \frac{-i}{\sqrt{n}} \\ 0 & 0 & 0 & 0 \end{pmatrix}, E^3 = \frac{1}{\sqrt{2}} \begin{pmatrix} 1 & 0 & 0 & -\frac{1}{n} \\ 0 & 1 & 0 & 0 \\ 0 & 0 & 1 & 0 \\ 0 & 0 & 0 & 1 \end{pmatrix}, \quad (\text{A14})$$

$$E_R^0 = \frac{1}{\sqrt{2}} \begin{pmatrix} \frac{1}{n} \\ 0 \\ 0 \\ 1 \end{pmatrix}, E_R^1 = \frac{1}{\sqrt{2}} \begin{pmatrix} 0 \\ \frac{1}{\sqrt{n}} \\ \frac{1}{\sqrt{n}} \\ 0 \end{pmatrix}, E_R^2 = \frac{1}{\sqrt{2}} \begin{pmatrix} 0 \\ i\frac{1}{\sqrt{n}} \\ -i\frac{1}{\sqrt{n}} \\ 0 \end{pmatrix}, E_R^3 = \frac{1}{\sqrt{2}} \begin{pmatrix} -\frac{1}{n} \\ 0 \\ 0 \\ 1 \end{pmatrix}, \quad (\text{A15})$$

so the SRE is

$$M_2(|W_n\rangle) = -\log \left[\left(\sum_{t=0}^3 E_L^t \otimes^4 \right) \left(\sum_{t=0}^3 E^t \otimes^4 \right)^{n-2} \left(\sum_{t=0}^3 E_R^t \otimes^4 \right) \right] - n \log 2 \quad (\text{A16})$$

$$= 3 \log n - \log(7n - 6). \quad (\text{A17})$$

where the calculation is performed using Mathematica.

3. Dicke states

The Dicke state is defined as

$$|D_k^n\rangle = \frac{1}{\sqrt{C_n^k}} \sum_i \mathcal{P}_i(|0\rangle^{\otimes n-k} \otimes |1\rangle^{\otimes k}) \quad (\text{A18})$$

where $k = 0, 1, \dots, n$ is the number of 1's, and the summation is over all distinct permutations, e.g., for $n = 4, k = 2$ we have

$$|D_2^4\rangle = \frac{|1100\rangle + |1010\rangle + |1001\rangle + |0110\rangle + |0101\rangle + |0011\rangle}{\sqrt{C_4^2}}, \quad (\text{A19})$$

and the W state we discussed above is actually a special Dicke state with $k = 1$,

$$|W_n\rangle = |D_1^n\rangle = \frac{|100\dots 0\rangle + |010\dots 0\rangle + |001\dots 0\rangle + \dots + |000\dots 1\rangle}{\sqrt{C_n^1}}. \quad (\text{A20})$$

For $k = 2$ Dicke states, we have

$$A_{L,1}^0 = \begin{pmatrix} 1 & 0 \end{pmatrix}, A_{L,1}^1 = \begin{pmatrix} 0 & a \end{pmatrix}, A_{L,2}^0 = \begin{pmatrix} 1 & 0 & 0 \\ 0 & 1 & 0 \end{pmatrix}, A_{L,2}^1 = \begin{pmatrix} 0 & a & 0 \\ 0 & 0 & 1 \end{pmatrix}, \quad (\text{A21})$$

$$A_{R,2}^0 = \begin{pmatrix} 0 & 0 \\ 1 & 0 \\ 0 & 1 \end{pmatrix}, A_{R,2}^1 = \begin{pmatrix} a & 0 \\ 0 & 1 \\ 0 & 0 \end{pmatrix}, A_{R,1}^0 = \begin{pmatrix} 0 \\ 1 \end{pmatrix}, A_{R,1}^1 = \begin{pmatrix} 1 \end{pmatrix}, \quad (\text{A22})$$

$$A^0 = \begin{pmatrix} 1 & 0 & 0 \\ 0 & 1 & 0 \\ 0 & 0 & 1 \end{pmatrix}, A^1 = \begin{pmatrix} 0 & a & 0 \\ 0 & 0 & 1 \\ 0 & 0 & 0 \end{pmatrix}. \quad (\text{A23})$$

where $a = (C_n^2)^{-1/2} = [n(n-1)/2]^{-1/2}$ is the normalization factor. Then the SRE is ($n \geq 4$)

$$M_2(|D_2^n\rangle) = -\log \left[\left(\sum_{t=0}^3 E_{L,1}^t \otimes^4 \right) \left(\sum_{t=0}^3 E_{L,2}^t \otimes^4 \right) \left(\sum_{t=0}^3 E^t \otimes^4 \right)^{n-4} \left(\sum_{t=0}^3 E_{R,2}^t \otimes^4 \right) \left(\sum_{t=0}^3 E_{R,1}^t \otimes^4 \right) \right] - n \log 2. \quad (\text{A24})$$

Denoting

$$D = \sum_{t=0}^3 (E^t)^{\otimes 4}, \quad (\text{A25})$$

one can find that the order of D is $3^4 = 6561$ thus making it quite slow for Mathematica to give an explicit expression of SRE. However, we can obtain the final result by using some tricks.

Suppose $P \in \mathcal{P}_n$ is a n -qubit Pauli string, the following equation yields

$$\langle P \rangle = \langle D_2^n | P | D_2^n \rangle = a^2 \sum_{i=1}^{n-1} \sum_{i'=i+1}^n \sum_{j=1}^{n-1} \sum_{j'=j+1}^n \langle 0|^{\otimes n} \hat{\sigma}_i^x \hat{\sigma}_{i'}^x P \hat{\sigma}_j^x \hat{\sigma}_{j'}^x | 0 \rangle^{\otimes n}, \quad (\text{A26})$$

and the $\|\Xi(|D_2^n\rangle)\|$ is

$$\|\Xi(|D_2^n\rangle)\| = \sum_{P \in \mathcal{P}_n} \frac{\langle P \rangle^4}{2^{2n}}, \quad (\text{A27})$$

therefore we first conclude that

$$\|\Xi(|D_2^n\rangle)\| = a^8 f(n) \quad (\text{A28})$$

where $f(n)$ is a function of n .

We denote $B^t = \sqrt{2}E^t = \sum_{s,s'=0}^1 \sigma_{s,s'}^t A^s \otimes \bar{A}^{s'}$ and set $a = 1$. Because we have already known the relation of $\|\Xi(|D_2^n\rangle)\|$ and a , so setting $a = 1$ has no effect on $f(n)$. Now all the A^s tensors are composed of 0s and 1s thus making B^t tensors composed of ± 1 and $\pm i$ as shown below.

$$B^0 = \mathbb{I} + X, B^1 = J + Y \quad (\text{A29})$$

$$B^3 = \mathbb{I} - X, B^2 = -i(J - Y) \quad (\text{A30})$$

where \mathbb{I} is identity and

$$(X)_{i,j} = \delta_{j-i,4} - \delta_{i,3}\delta_{j,7}, \quad 1 \leq i \leq 5, 5 \leq j \leq 9 \quad (\text{A31})$$

$$(J)_{i,j} = \delta_{j-i,1} - \delta_{i,3}\delta_{j,4} - \delta_{i,6}\delta_{j,7}, \quad 1 \leq i \leq 8, 2 \leq j \leq 9 \quad (\text{A32})$$

$$(Y)_{i,j} = \delta_{j-i,3}, \quad 1 \leq i \leq 6, 4 \leq j \leq 9. \quad (\text{A33})$$

We further calculate $(B^0)^{\otimes 4} + (B^3)^{\otimes 4}$ and find

$$(B^0)^{\otimes 4} + (B^3)^{\otimes 4} = (\mathbb{I} + X)^{\otimes 4} + (\mathbb{I} - X)^{\otimes 4} \quad (\text{A34})$$

$$= 2(\mathbb{I}^{\otimes 4} + \sum_{cyc} \mathbb{I}^{\otimes 2} X^{\otimes 2} + X^{\otimes 4}) \quad (\text{A35})$$

and similarly

$$(B^1)^{\otimes 4} + (B^2)^{\otimes 4} = (J + Y)^{\otimes 4} + (J - Y)^{\otimes 4} \quad (\text{A36})$$

$$= 2(J^{\otimes 4} + \sum_{cyc} J^{\otimes 2} Y^{\otimes 2} + Y^{\otimes 4}) \quad (\text{A37})$$

where \sum_{cyc} means sum over all possible permutations.

Therefore, it can be clearly seen that the matrix $\sum_{t=0}^3 (B^t)^{\otimes 4}$ is composed of 0s and 2s because there are only 0s and 1s in \mathbb{I}, X, J, Y and they satisfy $A_{i,j}B_{i,j} = 0, \forall i, j$ and thus we have

$$D = \sum_{t=0}^3 (E^t)^{\otimes 4} = \frac{1}{2} \left[\frac{1}{2} \sum_{t=0}^3 (B^t)^{\otimes 4} \right] := \frac{1}{2} T \quad (\text{A38})$$

where T is only composed of 0s and 1s. The calculation of $\|\Xi(|D_2^n\rangle)\|$ involves evaluating the matrix element of $D^n = 2^{-n} T^n$, so we second conclude that

$$\|\Xi(|D_2^n\rangle)\| = a^8 2^{-n} g(n) \quad (\text{A39})$$

where $g(n)$ is the combination of some of the matrix elements of T^n .

For T , we can decomposed it into the sum of an identity \mathbb{I} and a strict upper triangular matrix U

$$T = \mathbb{I} + U, \quad (\text{A40})$$

and by Cayley–Hamilton theorem, U is nilpotent, which means there exists a n_m such that

$$U^n = 0, \forall n \geq n_m. \quad (\text{A41})$$

Therefore for T^n , we can expand it as

$$T^n = (\mathbb{I} + U)^n = \sum_{k=0}^{\min(n, n_m-1)} C_n^k U^k = \mathbb{I} + C_n^1 U + C_n^2 U^2 + \dots \quad (\text{A42})$$

and the matrix element of $(T^n)_{i,j}$ is

$$(T^n)_{i,j} = \delta_{i,j} + C_n^1 U_{i,j} + C_n^2 (U^2)_{i,j} + \dots \quad (\text{A43})$$

where all of the matrix elements of U, U^2, \dots are independent of n as they are settled when U is given. Now, thirdly we conclude that the matrix elements of T^n must be polynomials in n , and so must $g(n)$.

Since we know $g(n)$ is a polynomial, instead of calculating T^n , it is easier to calculate the first few values of $g(n)$ and guess its expression. For example, we have the following terms for $g(n)$

$$\begin{aligned} g(4) &= 720, g(5) = 3160, g(6) = 9045, g(7) = 20601, \\ g(8) &= 40600, g(9) = 72360, g(10) = 119745, \dots \end{aligned} \quad (\text{A44})$$

and if you pay enough attention, you will notice that the fourth finite difference of this sequence is constant which is 546. This directly tells us $g(n)$ is a fourth-degree polynomial in n and its expression can be solved by those values above. The final result is

$$g(n) = \frac{1}{4}n(n-1)(91n^2 - 427n + 492). \quad (\text{A45})$$

and thus we obtain the analytical expression of $M_2(|D_2^n\rangle)$. We note that one can use this method to give analytical expression of 2-SRE of $k \geq 3$ Dicke states and we do provide the result of $k = 3$ Dicke state where $g(n)$ is sixth-degree polynomial.

Appendix B: Construction of MPO for bond-DMRG

We directly construct the MPO form of D . We now define new transfer matrices, which is basically E^t but with no $1/\sqrt{2}$ factor, i.e.,

$$B^t = \sqrt{2}E^t = \sum_{s,s'=0}^1 \sigma_{s,s'}^t A^s \otimes \bar{A}^{s'} \quad (\text{B1})$$

and the four B matrices can be clearly written,

$$B^0 = A^0 \otimes \bar{A}^0 + A^1 \otimes \bar{A}^1 \quad (\text{B2})$$

$$B^1 = A^0 \otimes \bar{A}^1 + A^1 \otimes \bar{A}^0 \quad (\text{B3})$$

$$B^2 = -iA^0 \otimes \bar{A}^1 + iA^1 \otimes \bar{A}^0 \quad (\text{B4})$$

$$B^3 = A^0 \otimes \bar{A}^0 - A^1 \otimes \bar{A}^1. \quad (\text{B5})$$

First define F^t as

$$F^0 = A^0 \otimes \bar{A}^0, F^1 = A^0 \otimes \bar{A}^1 \quad (\text{B6})$$

$$F^2 = A^1 \otimes \bar{A}^0, F^3 = A^1 \otimes \bar{A}^1 \quad (\text{B7})$$

and now we put B^0 and B^3 together,

$$(B^0)^{\otimes 4} + (B^3)^{\otimes 4} = (F^0 + F^3)^{\otimes 4} + (F^0 - F^3)^{\otimes 4} \quad (\text{B8})$$

$$\begin{aligned} &= 2 \left[(F^0)^{\otimes 4} + (F^3)^{\otimes 4} + F^0 \otimes F^0 \otimes F^3 \otimes F^3 \right. \\ &\quad + F^0 \otimes F^3 \otimes F^0 \otimes F^3 + F^0 \otimes F^3 \otimes F^3 \otimes F^0 \\ &\quad \left. + F^3 \otimes F^0 \otimes F^0 \otimes F^3 + F^3 \otimes F^0 \otimes F^3 \otimes F^0 + F^3 \otimes F^3 \otimes F^0 \otimes F^0 \right] \end{aligned} \quad (\text{B9})$$

and this term can be written in the MPO form with bond dimension 2,

$$\frac{1}{2} [(B^0)^{\otimes 4} + (B^3)^{\otimes 4}] = \begin{bmatrix} F^3 & F^0 \end{bmatrix} \begin{bmatrix} F^0 & F^3 \\ F^3 & F^0 \end{bmatrix} \begin{bmatrix} F^0 & F^3 \\ F^3 & F^0 \end{bmatrix} \begin{bmatrix} F^3 \\ F^0 \end{bmatrix} \quad (\text{B10})$$

and similarly for $(B^1)^{\otimes 4} + (B^2)^{\otimes 4}$ we have

$$\frac{1}{2} [(B^1)^{\otimes 4} + (B^2)^{\otimes 4}] = (F^1 + F^2)^{\otimes 4} + (F^1 - F^2)^{\otimes 4} \quad (\text{B11})$$

$$= \begin{bmatrix} F^2 & F^1 \end{bmatrix} \begin{bmatrix} F^1 & F^2 \\ F^2 & F^1 \end{bmatrix} \begin{bmatrix} F^1 & F^2 \\ F^2 & F^1 \end{bmatrix} \begin{bmatrix} F^2 \\ F^1 \end{bmatrix}. \quad (\text{B12})$$

Then the MPO representation of $4D = \sum_{t=0}^3 (B^t)^{\otimes 4}$ is

$$D = \frac{1}{4} \sum_{t=0}^3 (B^t)^{\otimes 4} = \frac{1}{2} \begin{bmatrix} F^3 & F^0 & F^2 & F^1 \end{bmatrix} \begin{bmatrix} F^0 & F^3 & 0 & 0 \\ F^3 & F^0 & 0 & 0 \\ 0 & 0 & F^1 & F^2 \\ 0 & 0 & F^2 & F^1 \end{bmatrix} \begin{bmatrix} F^0 & F^3 & 0 & 0 \\ F^3 & F^0 & 0 & 0 \\ 0 & 0 & F^1 & F^2 \\ 0 & 0 & F^2 & F^1 \end{bmatrix} \begin{bmatrix} F^3 \\ F^0 \\ F^2 \\ F^1 \end{bmatrix} \quad (\text{B13})$$

and further we can write the MPO of D in terms of A tensor with bond dimension no more than 8,

$$D = \frac{1}{2} \begin{bmatrix} 1 & 0 & 1 & 0 \end{bmatrix} \begin{bmatrix} \bar{1} & \cdot & \cdot & \cdot \\ \cdot & \bar{0} & \cdot & \cdot \\ \cdot & \cdot & \bar{0} & \cdot \\ \cdot & \cdot & \cdot & \bar{1} \end{bmatrix} \begin{bmatrix} 0 & 1 & \cdot & \cdot & \cdot & \cdot & \cdot & \cdot \\ \cdot & \cdot & 1 & 0 & \cdot & \cdot & \cdot & \cdot \\ \cdot & \cdot & \cdot & \cdot & 0 & 1 & \cdot & \cdot \\ \cdot & \cdot & \cdot & \cdot & \cdot & \cdot & 1 & 0 \end{bmatrix} \begin{bmatrix} \bar{0} & \cdot & \cdot & \cdot \\ \cdot & \bar{1} & \cdot & \cdot \\ \bar{1} & \cdot & \cdot & \cdot \\ \cdot & \bar{0} & \cdot & \cdot \\ \cdot & \cdot & \bar{1} & \cdot \\ \cdot & \cdot & \cdot & \bar{0} \\ \cdot & \cdot & \bar{0} & \cdot \\ \cdot & \cdot & \cdot & \bar{1} \end{bmatrix} \begin{bmatrix} 0 & 1 & \cdot & \cdot & \cdot & \cdot & \cdot & \cdot \\ \cdot & \cdot & 1 & 0 & \cdot & \cdot & \cdot & \cdot \\ \cdot & \cdot & \cdot & \cdot & 0 & 1 & \cdot & \cdot \\ \cdot & \cdot & \cdot & \cdot & \cdot & \cdot & 1 & 0 \end{bmatrix} \begin{bmatrix} \bar{0} & \cdot & \cdot & \cdot \\ \cdot & \bar{1} & \cdot & \cdot \\ \bar{1} & \cdot & \cdot & \cdot \\ \cdot & \bar{0} & \cdot & \cdot \\ \cdot & \cdot & \bar{1} & \cdot \\ \cdot & \cdot & \cdot & \bar{0} \\ \cdot & \cdot & \bar{0} & \cdot \\ \cdot & \cdot & \cdot & \bar{1} \end{bmatrix} \begin{bmatrix} 1 & \cdot & \cdot & \cdot \\ \cdot & 0 & \cdot & \cdot \\ \cdot & \cdot & 1 & \cdot \\ \cdot & \cdot & \cdot & 0 \end{bmatrix} \begin{bmatrix} \bar{1} \\ \bar{0} \\ \bar{0} \\ \bar{1} \end{bmatrix} \quad (\text{B14})$$

where we use $0, 1, \bar{0}, \bar{1}$ to represent A^0, A^1, \bar{A}^0 and \bar{A}^1 , and \cdot for zero matrix, respectively.

Appendix C: Asymptotic behaviour of two-site mutual SRE in the injective TIMPS

The stabilizer Rényi entropy $\tilde{M}_2(\rho)$ can be extended to mixed states, defined as

$$\tilde{M}_2(\rho) := M_2(\rho) - S_2(\rho) \quad (\text{C1})$$

with $S_2(\rho)$ the 2-Rényi entropy of ρ and

$$M_2(\rho) = -\log \text{tr}(Q_n \rho^{\otimes 4}) - \log d. \quad (\text{C2})$$

where $Q_n = d^{-2} \sum_{P \in \mathcal{P}_n} P^{\otimes 4}$.

The long-range magic can thus be quantified by

$$L(\rho_{AB}) = \tilde{M}_2(\rho_{AB}) - \tilde{M}_2(\rho_A) - \tilde{M}_2(\rho_B). \quad (\text{C3})$$

which consists of two parts

$$L(\rho_{AB}) = L_M(\rho_{AB}) + L_S(\rho_{AB}), \quad (\text{C4})$$

$$L_M(\rho_{AB}) := M_2(\rho_{AB}) - M_2(\rho_A) - M_2(\rho_B), \quad (\text{C5})$$

$$L_S(\rho_{AB}) := S_2(\rho_A) + S_2(\rho_B) - S_2(\rho_{AB}). \quad (\text{C6})$$

We first calculate the Rényi entropy part. Suppose there are r sites between A and B (and the site of A and B are denoted as s_1, s_2 , and we have $s_2 - s_1 - 1 = m$), then the density matrix of joint system AB is

$$\rho_{AB} = (l|(A^{s_1} \otimes \bar{A}^{s'_1})(E_A^{\bar{A}})^r(A^{s_2} \otimes \bar{A}^{s'_2})|r), \quad (\text{C7})$$

using the eigendecomposition of transfer matrix $E_A^{\bar{A}}$,

$$E_A^{\bar{A}} = |r)(l| + \sum_i \lambda_i |\lambda_i)(\lambda_i| \quad (\text{C8})$$

we obtain

$$\rho_{AB} = (l|(A^{s_1} \otimes \bar{A}^{s'_1})|r) \otimes (l|(A^{s_2} \otimes \bar{A}^{s'_2})|r) + \sum_i \lambda_i^r (l|(A^{s_1} \otimes \bar{A}^{s'_1})|\lambda_i) \otimes (\lambda_i|(A^{s_2} \otimes \bar{A}^{s'_2})|r) \quad (\text{C9})$$

denoting

$$\rho_l(\lambda_i) = (l|(A^{s_1} \otimes \bar{A}^{s'_1})|\lambda_i) \quad (\text{C10})$$

$$\rho_r(\lambda_i) = (\lambda_i|(A^{s_2} \otimes \bar{A}^{s'_2})|r) \quad (\text{C11})$$

the above equation is simplified to

$$\rho_{AB} = \rho_A \otimes \rho_B + \sum_i \lambda_i^r \rho_l(\lambda_i) \otimes \rho_r(\lambda_i). \quad (\text{C12})$$

Now we try to calculate the Rényi entropy of ρ_{AB} , first we square ρ_{AB}

$$\begin{aligned} \rho_{AB}^2 &= \rho_A^2 \otimes \rho_B^2 + \left(\sum_i \lambda_i^r \rho_A \rho_l(\lambda_i) \otimes \rho_B \rho_r(\lambda_i) \right) + \left(\sum_i \lambda_i^r \rho_l(\lambda_i) \rho_A \otimes \rho_r(\lambda_i) \rho_B \right) \\ &\quad + \left(\sum_{i,j} \lambda_i^r \lambda_j^r \rho_l(\lambda_i) \rho_l(\lambda_j) \otimes \rho_r(\lambda_i) \rho_r(\lambda_j) \right) \end{aligned} \quad (\text{C13})$$

then trace it,

$$\text{tr}(\rho_{AB}^2) = \text{tr}(\rho_A^2) \text{tr}(\rho_B^2) + 2 \sum_i \lambda_i^r \text{tr}[\rho_A \rho_l(\lambda_i)] \text{tr}[\rho_B \rho_r(\lambda_i)] + \sum_{i,j} \lambda_i^r \lambda_j^r \text{tr}[\rho_l(\lambda_i) \rho_l(\lambda_j)] \text{tr}[\rho_r(\lambda_i) \rho_r(\lambda_j)] \quad (\text{C14})$$

we now obtain the Rényi entropy of ρ_{AB}

$$S_2(\rho_{AB}) = -\log [\text{tr}(\rho_{AB}^2)] \quad (\text{C15})$$

and the expression for $L_S(\rho_{AB})$ is

$$L_S(\rho_{AB}) = -2 \log [\text{tr}(\rho_A^2)] + \log [\text{tr}(\rho_{AB}^2)] \quad (\text{C16})$$

$$= \log \left[1 + 2 \sum_i \lambda_i^r \frac{\text{tr}[\rho_A \rho_l(\lambda_i)] \text{tr}[\rho_A \rho_r(\lambda_i)]}{\text{tr}(\rho_A^2)^2} + \sum_{i,j} \lambda_i^r \lambda_j^r \frac{\text{tr}[\rho_l(\lambda_i) \rho_l(\lambda_j)] \text{tr}[\rho_r(\lambda_i) \rho_r(\lambda_j)]}{\text{tr}(\rho_A^2)^2} \right], \quad (\text{C17})$$

thus in the long-range limit $r \rightarrow +\infty$ we obtain

$$L_S(\rho_{AB}) \sim \log [1 + 2\lambda_1^r c_s] \quad (\text{C18})$$

where c_s is a constant

$$c_s = \frac{\text{tr}[\rho_A \rho_l(\lambda_1)] \text{tr}[\rho_A \rho_r(\lambda_1)]}{\text{tr}(\rho_A^2)^2}. \quad (\text{C19})$$

As for the stabilizer Rényi entropy part $L_M(\rho_{AB})$, we first simplify it

$$L_M(\rho_{AB}) = -\log \text{tr}(Q_2 \rho_{AB}^{\otimes 4}) - \log 2^2 - 2(-\log \text{tr}(Q_1 \rho_A^{\otimes 4}) - \log 2) \quad (\text{C20})$$

$$= -\log \frac{\text{tr}(Q_2 \rho_{AB}^{\otimes 4})}{\text{tr}(Q_1 \rho_A^{\otimes 4})^2} \quad (\text{C21})$$

and we begin from Eq. (C12),

$$\text{tr}(Q_2 \rho_{AB}^{\otimes 4}) = \sum_{t,t'} \left[\text{tr}(\rho_A U^t) \text{tr}(\rho_A U^{t'}) + \sum_i \lambda_i^r \text{tr}(\rho_l(\lambda_i) U^t) \text{tr}(\rho_r(\lambda_i) U^{t'}) \right]^4 \quad (\text{C22})$$

where $U_{s,s'}^t = \sigma_{s,s'}^t / \sqrt{2}$, and then

$$L_M(\rho_{AB}) = -\log \frac{\sum_{t,t'} \left[\text{tr}(\rho_A U^t) \text{tr}(\rho_A U^{t'}) + \sum_i \lambda_i^r \text{tr}(\rho_l(\lambda_i) U^t) \text{tr}(\rho_r(\lambda_i) U^{t'}) \right]^4}{\sum_{t,t'} \text{tr}(\rho_A U^t)^4 \text{tr}(\rho_A U^{t'})^4} \quad (\text{C23})$$

which directly gives

$$\begin{aligned} L_M(\rho_{AB}) &= -\log \left[1 + \frac{4 \sum_{t,t'} (A^{tt'})^3 \sum_i \lambda_i^{tt'} + 6 \sum_{t,t'} (A^{tt'})^2 (\sum_i \lambda_i^{tt'})^2 + 4 \sum_{t,t'} A^{tt'} (\sum_i \lambda_i^{tt'})^3 + (\sum_i \lambda_i^{tt'})^4}{\sum_{t,t'} (A^{tt'})^4} \right] \\ &= -\log \left[1 + 4 \sum_{t,t'} a_1^{tt'} \lambda^{tt'} + 6 \sum_{t,t'} a_2^{tt'} (\lambda^{tt'})^2 + 4 \sum_{t,t'} a_3^{tt'} (\lambda^{tt'})^3 + \sum_{t,t'} (\lambda^{tt'})^4 \right] \end{aligned} \quad (\text{C24})$$

where we use the following notations for simplicity

$$A^{tt'} = \text{tr}(\rho_A U^t) \text{tr}(\rho_A U^{t'}) \quad (\text{C25})$$

$$a_k^{tt'} = \frac{(A^{tt'})^{4-k}}{\sum_{t,t'} (A^{tt'})^4} \quad (\text{C26})$$

$$\lambda_i^{tt'} = \lambda_i^r \text{tr}(\rho_l(\lambda_i) U^t) \text{tr}(\rho_r(\lambda_i) U^{t'}) \quad (\text{C27})$$

$$\lambda^{tt'} = \sum_i \lambda_i^{tt'} \quad (\text{C28})$$

and in the long-range limit $r \rightarrow +\infty$, the above expression gives

$$L_M(\rho_{AB}) \sim -\log[1 + 4 \sum_{t,t'} a_1^{tt'} \lambda_1^{tt'}] \quad (\text{C29})$$

$$\sim -\log \left[1 + 4 \lambda_1^r \sum_{t,t'} a_1^{tt'} \text{tr}(\rho_l(\lambda_1) U^t) \text{tr}(\rho_r(\lambda_1) U^{t'}) \right] \quad (\text{C30})$$

$$\sim -\log[1 + 2 \lambda_1^r c_m] \quad (\text{C31})$$

where $c_m = 2 \sum_{t,t'} a_1^{tt'} \text{tr}(\rho_l(\lambda_1) U^t) \text{tr}(\rho_r(\lambda_1) U^{t'})$ is a constant. Then the mutual SRE of any injective TIMPS in the long-range limit is given by ($0 \leq |\lambda_1| < 1$, r is the distance between two subsystems)

$$\lim_{r \rightarrow +\infty} L(\rho_{AB}) = \lim_{r \rightarrow +\infty} \log \left[\frac{1 + 2 \lambda_1^r c_m}{1 + 2 \lambda_1^r c_m} \right] = 0. \quad (\text{C32})$$

Here, we note that λ_1 is directly related to the correlation length ξ by the following relation

$$\xi = -\frac{1}{\ln |\lambda_1|}. \quad (\text{C33})$$

Other behaviour of long-range magic can be more accurately evaluated

$$L(\rho_{AB}) \sim \log \left[\frac{1 + 2 \sum_i \lambda_i^r c_i}{1 + 4 \sum_i \lambda_i^r d_i} \right] \quad (\text{C34})$$

where

$$c_i = \frac{\text{tr}[\rho_A \rho_l(\lambda_i)] \text{tr}[\rho_A \rho_r(\lambda_i)]}{\text{tr}(\rho_A^2)^2}, \quad (\text{C35})$$

$$d_i = \sum_{t,t'} a_1^{tt'} \text{tr}(\rho_l(\lambda_i) U^t) \text{tr}(\rho_r(\lambda_i) U^{t'}). \quad (\text{C36})$$

Appendix D: Calculation of two-point mutual SRE in Ising model

We consider the following transverse field Ising model (TFIM)

$$\hat{H}_{\text{TFIM}} = -h \sum_i \hat{\sigma}_i^x - J \sum_i \hat{\sigma}_i^z \hat{\sigma}_{i+1}^z \quad (\text{D1})$$

and perform local unitary transformation,

$$\hat{H}'_{\text{TFIM}} = -h \sum_i \hat{H}_i \hat{\sigma}_i^x \hat{H}_i - J \sum_i \hat{H}_i \hat{\sigma}_i^z \hat{H}_i \hat{H}_{i+1} \hat{\sigma}_{i+1}^z \hat{H}_{i+1} \quad (\text{D2})$$

$$= -h \sum_i \hat{\sigma}_i^z - J \sum_i \hat{\sigma}_i^x \hat{\sigma}_{i+1}^x \quad (\text{D3})$$

where \hat{H} is a Hadamard gate

$$\hat{H}_i = \frac{\hat{\sigma}_i^z + \hat{\sigma}_i^x}{\sqrt{2}}, \quad (\text{D4})$$

and it satisfies $\hat{H}^\dagger = \hat{H}^{-1} = \hat{H}$.

The Hadamard gate is a Clifford operation, so the mSRE in model described by \hat{H}'_{TFIM} has no difference with the one in \hat{H}_{TFIM} . We focus on the second Ising model \hat{H}'_{TFIM} in the following.

The Hamiltonian \hat{H}'_{TFIM} can be exactly solved by Jordan-Wigner transformation. The Hamiltonian written in fermion operators is

$$\hat{H}'_{\text{TFIM}} = h \sum_j (2\hat{c}_j^\dagger \hat{c}_j - 1) - J \sum_j (\hat{c}_j^\dagger \hat{c}_{j+1} + \hat{c}_j^\dagger \hat{c}_{j+1}^\dagger + h.c.), \quad (\text{D5})$$

and using Fourier transformation,

$$\hat{c}_k = \frac{1}{\sqrt{L}} \sum_j e^{-ikj} \hat{c}_j \quad (\text{D6})$$

$$\hat{c}_j = \frac{1}{\sqrt{L}} \sum_k e^{ikj} \hat{c}_k \quad (\text{D7})$$

we obtain the Hamiltonian in momentum space

$$\hat{H}'_{\text{TFIM}} = \begin{pmatrix} \hat{c}_k^\dagger & \hat{c}_{-k} \end{pmatrix} \begin{pmatrix} 2(h - J \cos k) & -i2J \sin k \\ i2J \sin k & -2(h - J \cos k) \end{pmatrix} \begin{pmatrix} \hat{c}_k \\ \hat{c}_{-k}^\dagger \end{pmatrix} \quad (\text{D8})$$

thus we can directly diagonalize the Hamiltonian and obtain the energy spectrum $\epsilon_{k\pm} = \pm \epsilon_k$

$$\epsilon_k = 2J \sqrt{\left(\frac{h}{J} - \cos k \right)^2 + \sin^2 k} \quad (\text{D9})$$

with corresponding eigenvectors $(v_{k\pm}, u_{k\pm})^T$

$$\begin{pmatrix} v_{k-} \\ u_{k-} \end{pmatrix} = \begin{pmatrix} v_k \\ u_k \end{pmatrix} = \frac{1}{\sqrt{2\epsilon_k(\epsilon_k + z_k)}} \begin{pmatrix} iy_k \\ \epsilon_k + z_k \end{pmatrix} \quad (\text{D10})$$

$$\begin{pmatrix} v_{k+} \\ u_{k+} \end{pmatrix} = \begin{pmatrix} u_k^* \\ -v_k^* \end{pmatrix} = \frac{1}{\sqrt{2\epsilon_k(\epsilon_k + z_k)}} \begin{pmatrix} \epsilon_k + z_k \\ iy_k \end{pmatrix} \quad (\text{D11})$$

where we define $y_k = 2J \sin k$ and $z_k = 2(h - J \cos k)$. Now we can explicitly write the ground state of the Ising model,

$$|\psi_0\rangle = \prod_{k>0} (u_k + v_k \hat{c}_k^\dagger \hat{c}_{-k}^\dagger) |0\rangle \quad (\text{D12})$$

where $|0\rangle$ is the vacuum state for fermions.

To calculate the two-point mSRE, we first calculate the two-point density matrix which can be expressed as

$$\rho_{ij} = \sum_{\alpha, \beta=0}^3 R_{\alpha\beta} \hat{\sigma}_i^\alpha \hat{\sigma}_j^\beta. \quad (\text{D13})$$

Due to the global \mathbb{Z}_2 symmetry of Ising model Hamiltonian \hat{H}'_{TFIM} , the coefficients of the terms like $\sigma_i^x \sigma_j^z$ which anti-commute with $\hat{F} = \prod_j \hat{\sigma}_j^z$ should be zero. This is because the system's symmetry requires, if there is no spontaneous symmetry breaking, the two-point density matrix should be invariant under the global \mathbb{Z}_2 transformation, which is

$$\hat{F} \rho_{ij} \hat{F}^\dagger = \rho_{ij} \Rightarrow [\hat{F}, \rho_{ij}] = 0. \quad (\text{D14})$$

Therefore, the R_α matrix has the following form

$$R_{\alpha\beta} = \frac{1}{4} \begin{pmatrix} 1 & 0 & 0 & \langle \hat{\sigma}_i^z \rangle \\ 0 & \langle \hat{\sigma}_i^x \hat{\sigma}_j^x \rangle & 0 & 0 \\ 0 & 0 & \langle \hat{\sigma}_i^y \hat{\sigma}_j^y \rangle & 0 \\ \langle \hat{\sigma}_j^z \rangle & 0 & 0 & \langle \hat{\sigma}_i^z \hat{\sigma}_j^z \rangle \end{pmatrix}. \quad (\text{D15})$$

We note that there is no $\sigma_i^x \sigma_j^y$ term because the TFIM Hamiltonian is also invariant under time-reversal operation denoted $T = K$ and $[K, \sigma_i^x \sigma_j^y] \neq 0$ where K is the complex conjugation operator.

Similarly, the single-point density matrix can be expressed as

$$\rho_i = \frac{1}{2} (\mathbb{I} + \langle \hat{\sigma}_i^z \rangle \hat{\sigma}_i^z). \quad (\text{D16})$$

Now we only need to calculate the correlation functions $\langle \sigma_i^x \sigma_j^x \rangle, \langle \sigma_i^y \sigma_j^y \rangle, \langle \sigma_i^z \sigma_j^z \rangle$ and average value of σ_i^z . Define the one-particle Green's functions as follows

$$G_{jj'} = \langle \psi_0 | \hat{c}_j \hat{c}_{j'}^\dagger | \psi_0 \rangle, \quad (\text{D17})$$

$$F_{jj'} = \langle \psi_0 | \hat{c}_j \hat{c}_{j'} | \psi_0 \rangle, \quad (\text{D18})$$

in the thermodynamic limit, we have

$$G_{jj'} = \int_0^\pi \frac{dk}{2\pi} \frac{z_k}{\epsilon_k} \cos[k(j-j')] + \frac{1}{2} \delta_{j,j'} \quad (\text{D19})$$

$$F_{jj'} = \int_0^\pi \frac{dk}{2\pi} \frac{y_k}{\epsilon_k} \sin[k(j-j')]. \quad (\text{D20})$$

Using the above Green's functions combined with Wick theorem, we can obtain exact values of correlation functions.

Here we directly provide the results and for technical details, please refer to [55],

$$\langle \hat{\sigma}_i^z \rangle = 2 \left(G_{i,i} - \frac{1}{2} \right) \quad (\text{D21})$$

$$\langle \hat{\sigma}_i^z \hat{\sigma}_j^z \rangle = 4 \left(G_{i,i} - \frac{1}{2} \right) \left(G_{j,j} - \frac{1}{2} \right) + 4G_{i,j}(\delta_{i,j} - G_{j,i}) + 4|F_{i,j}|^2 \quad (\text{D22})$$

$$\langle \hat{\sigma}_i^x \hat{\sigma}_j^x \rangle = \det \begin{pmatrix} M_{i,i+1} & M_{i,i+2} & \cdots & M_{i,j} \\ M_{i+1,i+1} & M_{i+1,i+2} & \cdots & M_{i+1,j} \\ \vdots & \vdots & \ddots & \vdots \\ M_{j-2,i+1} & M_{j-2,i+2} & \cdots & M_{j-2,j} \\ M_{j-1,i+1} & M_{j-1,i+2} & \cdots & M_{j-1,j} \end{pmatrix} \quad (\text{D23})$$

$$\langle \hat{\sigma}_i^y \hat{\sigma}_j^y \rangle = \det \begin{pmatrix} M_{i+1,i} & M_{i+1,i+1} & \cdots & M_{i+1,j-1} \\ M_{i+2,i} & M_{i+2,i+1} & \cdots & M_{i+2,j-1} \\ \vdots & \vdots & \ddots & \vdots \\ M_{j-1,i} & M_{j-1,i+1} & \cdots & M_{j-1,j-1} \\ M_{j,i} & M_{j,i+1} & \cdots & M_{j,j-1} \end{pmatrix} \quad (\text{D24})$$

where $M_{i,j}$ is defined as

$$M_{i,j} = \delta_{i,j} - 2(G_{i,j} + F_{i,j}). \quad (\text{D25})$$

Using the above results, we can give exact values of two-point mutual SRE in the TFIM.